

In colony allore cognition assays, three of four isogenic pairs receiving control morpholinos fused within 24 hours of ampullae contact. By contrast, no reactions were observed in isogenic pairs receiving BHF translation-blocking morpholinos ($n = 6$), despite constant physical contact over observational periods ranging from 2 to 7 days (Fig. 3D, fig. S19, and table S8). To exclude nonspecific effects, we also tested BHF splice-inhibiting morpholinos, using the progeny of wild-type colonies (15). Within 2 days of ampullae contact, all control pairs had fused ($n = 2$) or rejected ($n = 1$), whereas colony pairs receiving splice-inhibiting morpholinos did not react ($n = 5$) (figs. S20 and S21, table S9, and movies S1 and S2). These data support our genomic analysis and indicate that BHF participates in fusion and rejection initiation.

In the jawed vertebrates, the MHC is a haplotype, each sublocus of which specifies a different recognition process, usually by unique subsets of cells (18–20). By contrast, the *B. schlosseri* Fu/HC locus is a single gene (*BHF*) embedded in a haplotype of several genes with high polymorphism. Unlike the secreted (*sFuHC*) and membrane-bound (*mFuHC*) genes, *BHF* has none of the domains expected for a cell surface–recognition protein or, in fact, domains that are conserved throughout protein evolution. Because *BHF* does not follow biological precedence by either sequence or domains, future investigations of this gene will likely reveal new mechanisms of recognition.

The ability to reliably predict histocompatibility outcomes on the basis of a single gene has broad implications for the study of allore cognition. For example, after vasculature fusion, stem cells from each *B. schlosseri* colony compete to overtake germline and/or somatic lineages (21–24). Stem cell competition may lead to elimination of

the other colony's genome or may produce a chimeric colony with mixed genotypes. To date, induction of chimerism using hematopoietic stem-cell transplantation is the only way to achieve long-term donor-specific tolerance to human organ allografts (25). Chimerism can be short-lived, and if lost, the threat of allograft rejection emerges. *B. schlosseri* is a unique species for studying stem cell–mediated chimerism, and such research will be facilitated by BHF.

References and Notes

- A. Nakashima, T. Shima, K. Inada, M. Ito, S. Saito, *Am. J. Reprod. Immunol.* **67**, 304 (2012).
- G. Girardi, Z. Prohászka, R. Bulla, F. Tedesco, S. Scherjon, *Mol. Immunol.* **48**, 1621 (2011).
- M. Colonna, S. Jonjic, C. Watzl, *Nat. Immunol.* **12**, 107 (2011).
- D. F. LaRosa, A. H. Rahman, L. A. Turka, *J. Immunol.* **178**, 7503 (2007).
- F. Delsuc, H. Brinkmann, D. Chourrout, H. Philippe, *Nature* **439**, 965 (2006).
- H. Oka, H. Watanabe, *Proc. Jpn. Acad. Ser. B* **33**, 657 (1957).
- H. Oka, H. Watanabe, *Bull. Mar. Biol. Stat. Asamushi* **10**, 153 (1960).
- A. Sabbadin, *Rend. Accad. Naz. Lincei. Ser.* **32**, 1031 (1962).
- V. L. Scofield, J. M. Schlumpberger, L. A. West, I. L. Weissman, *Nature* **295**, 499 (1982).
- A. W. De Tomaso, Y. Saito, K. J. Ishizuka, K. J. Palmeri, I. L. Weissman, *Genetics* **149**, 277 (1998).
- A. W. De Tomaso, I. L. Weissman, *Immunogenetics* **55**, 480 (2003).
- A. W. De Tomaso *et al.*, *Nature* **438**, 454 (2005).
- A. Voskoboinik *et al.*, *eLife* **2**, e00569 (2013).
- I. Letinic, T. Doerk, P. Bork, SMART 7: recent updates to the protein domain annotation resource. *Nucleic Acids Res.* **40**, D302 and (2012).
- Materials and methods are available as supplementary materials on *Science Online*.
- B. Rinkevich, J. Douek, C. Rabinowitz, G. Paz, *Dev. Comp. Immunol.* **36**, 718 (2012).
- M. Oren, J. Douek, Z. Fishelson, B. Rinkevich, *Dev. Comp. Immunol.* **31**, 889 (2007).
- The MHC sequencing consortium, *Nature* **401**, 921 (1999).
- M. Hirano, S. Das, P. Guo, M. D. Cooper, *Adv. Immunol.* **109**, 125 (2011).

- L. J. Dishaw, G. W. Litman, *Curr. Biol.* **19**, R286 (2009).
- D. S. Stoner, I. L. Weissman, *Proc. Natl. Acad. Sci. U.S.A.* **93**, 15254 (1996).
- D. S. Stoner, B. Rinkevich, I. L. Weissman, *Proc. Natl. Acad. Sci. U.S.A.* **96**, 9148 (1999).
- D. J. Laird, A. W. De Tomaso, I. L. Weissman, *Cell* **123**, 1351 (2005).
- A. Voskoboinik *et al.*, *Cell Stem Cell* **3**, 456 (2008).
- D. H. Sachs, M. Sykes, T. Kawai, A. B. Cosimi, *Semin. Immunol.* **23**, 165 (2011).

Acknowledgments: We thank B. Rinkevich for pointing out the difficulty with the original cFuHC assignments and T. Snyder, J. Okamoto, L. Me, L. Ooi, A. Dominguez, C. Lowe, K. Uhlinger, L. Crowder, S. Kartan, C. Patton, L. Jerabek, and T. Storm for invaluable technical advice and help. A. De Tomaso provided the fosmid sequence used to characterize cFuHC (12) (table S5). D.P., A.V., and S.R.Q. have filed U.S. and international patent applications (61/532,882 and 13/608,778, respectively) entitled "Methods for obtaining a sequence." This invention allows for the sequencing of long continuous (kilobase scale) nucleic acid fragments using conventional short read–sequencing technologies, useful for consensus sequencing and haplotype determination. This study was supported by NIH grants 1R56AI089968, R01GM100315, and R01AG037968 awarded to I.L.W., A.V., and S.R.Q., respectively, and the Virginia and D. K. Ludwig Fund for Cancer Research awarded to I.L.W. D.S. was supported by NIH grant K99CA151673-01A1 and Department of Defense Grant W81XWH-10-1-0500, and A.M.N., D.M.C., D.S., and I.K.D. were supported by a grant from the Siebel Stem Cell Institute and the Thomas and Stacey Siebel Foundation. The data in this paper are tabulated in the main manuscript and in the supplementary materials. BHF, sFuHC, and mFuHC sequences are available in GenBank under accession numbers KF017887-KF017889, and the RNA-Seq data are available on the Sequence Read Archive (SRA) database: BioProject SRP022042.

Supplementary Materials

www.sciencemag.org/cgi/content/full/341/6144/384/DC1

Materials and Methods

Figs. S1 to S21

Tables S1 to S9

References (26–42)

Movies S1 and S2

19 March 2013; accepted 30 May 2013

10.1126/science.1238036

whether these internal representations can be combined with external stimuli to generate new memories has not been vigorously studied.

Damage to the hippocampus impairs episodic memory (3–8). Recently, using fear conditioning in mice as a model of episodic memory, we identified a small subpopulation of granule cells in the dentate gyrus (DG) of the hippocampus as contextual memory-gram cells. Optogenetic stimulation of these cells is sufficient to activate behavioral recall of a context-dependent fear memory formed by a delivery of foot shocks. This finding provided an opportunity to investigate how the internal representation of a specific context can be associated with external stimuli of high valence. In particular, a hypothesis of great interest is

Creating a False Memory in the Hippocampus

Steve Ramirez,^{1*} Xu Liu,^{1,2*} Pei-Ann Lin,¹ Junghyup Suh,¹ Michele Pignatelli,¹ Roger L. Redondo,^{1,2} Tomás J. Ryan,^{1,2} Susumu Tonegawa^{1,2†}

Memories can be unreliable. We created a false memory in mice by optogenetically manipulating memory engram-bearing cells in the hippocampus. Dentate gyrus (DG) or CA1 neurons activated by exposure to a particular context were labeled with channelrhodopsin-2. These neurons were later optically reactivated during fear conditioning in a different context. The DG experimental group showed increased freezing in the original context, in which a foot shock was never delivered. The recall of this false memory was context-specific, activated similar downstream regions engaged during natural fear memory recall, and was also capable of driving an active fear response. Our data demonstrate that it is possible to generate an internally represented and behaviorally expressed fear memory via artificial means.

Neuroscience aims to explain how brain activity drives cognition. Doing so requires identification of the brain regions that are specifically involved in producing internal mental representations and perturbing their activity to

see how various cognitive processes are affected. More specifically, humans have a rich repertoire of mental representations generated internally by processes such as conscious or unconscious recall, dreaming, and imagination (1, 2). However,

¹RIKEN–Massachusetts Institute of Technology (MIT) Center for Neural Circuit Genetics at the Picower Institute for Learning and Memory, Department of Biology and Department of Brain and Cognitive Sciences, MIT, Cambridge, MA 02139, USA. ²Howard Hughes Medical Institute, MIT, Cambridge, MA 02139, USA.

*These authors contributed equally to this work.

†Corresponding author. E-mail: tonegawa@mit.edu

whether artificially activating a previously formed contextual memory engram while simultaneously delivering foot shocks can result in the creation of a false fear memory for the context in which foot shocks were never delivered. To address this, we investigated whether a light-activated contextual memory in the DG or CA1 can serve as a functional conditioned stimulus (CS) in fear conditioning.

Our system uses *c-fos-tTA* transgenic mice, in which the promoter of the *c-fos* gene drives the expression of the tetracycline transactivator (tTA) to induce expression of a gene of interest downstream of the tetracycline-responsive element (TRE) (8–12). We injected an adeno-associated virus (AAV) encoding TRE-ChR2-mCherry into the DG or CA1 of *c-fos-tTA* animals (Fig. 1A). Channelrhodopsin-2 (ChR2)-mCherry expression was completely absent in the DG of animals that had been raised with doxycycline (Dox) in the diet (on Dox) (Fig. 1B). Exploration of a novel context under the condition of Dox withdrawal (off Dox) elicited an increase in ChR2-mCherry expression (Fig. 1C). We confirmed the functionality of the expressed ChR2-mCherry by recording light-induced spikes in cells expressing ChR2-mCherry from both acute hippocampal slices and in anaesthetized animals (Fig. 1, D to

F). Furthermore, optical stimulation of ChR2-mCherry-expressing DG cells induced cFos expression throughout the anterior-posterior axis of the DG (fig. S1, A to I).

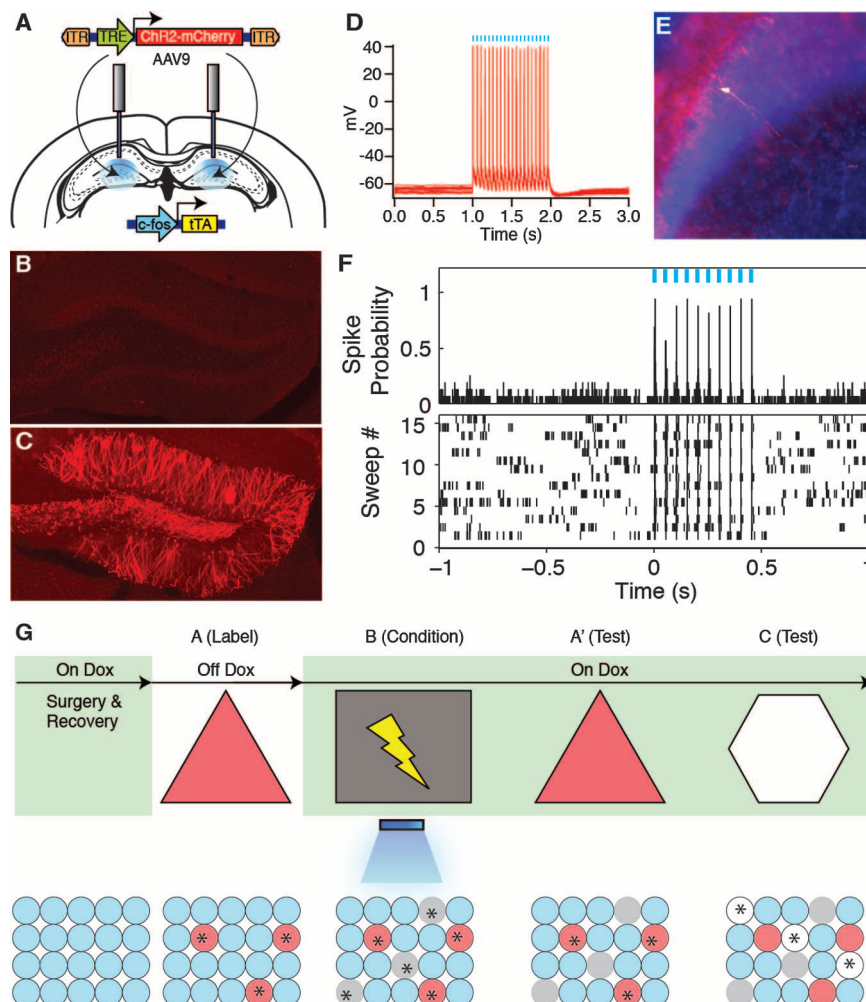
We first took virus-infected and fiber-implanted animals off Dox to open a time window for labeling cells activated by the exploration of a novel context (context A) with ChR2-mCherry. The animals were then put back on Dox to prevent any further labeling. The next day, we fear-conditioned this group in a distinct context (context B) while optically reactivating the cells labeled in context A. On the following 2 days, we tested the animals' fear memory in either the original context A or a novel context C (Fig. 1G). If the light-reactivated cells labeled in context A can produce a functional CS during fear conditioning in context B, then the animals should express a false fear memory by freezing in context A, but not in context C.

First, we examined the degree of overlap of the cell populations activated in contexts A and C (8, 11). We injected a group of *c-fos-tTA* mice with an AAV virus encoding TRE-ChR2-mCherry and exposed them to context A while off Dox so as to label activated DG cells with ChR2-mCherry. These animals were then immediately placed back on Dox to prevent further labeling. The next day,

half of the animals were exposed to context C, and the other half were reexposed to context A as a control. Both groups were euthanized 1.5 hours later. DG cells activated by the first exposure to context A were identified by ChR2-mCherry expression, and cells activated by the exposure to context C or the reexposure to context A were identified by the expression of endogenous c-Fos. The c-Fos generated by the first exposure to context A had been degraded by the time the animals underwent their second context exposure (11). Contexts A and C recruited statistically independent populations of DG cells. In contrast, two exposures to context A recruited substantially overlapping cell populations in the dorsal DG (Fig. 2, A to E).

When DG cells activated by the exposure to context A were reactivated with light during fear conditioning in a distinct context B, the animals subsequently froze in context A at levels significantly higher than the background levels, whereas freezing in context C did not differ from background levels (Fig. 2F). This increased freezing in context A was not due to generalization, because a control group expressing only mCherry that underwent the exact same training protocol did not show the same effect (Fig. 2F). A separate group of animals expressing ChR2-enhanced yellow fluorescent protein

Fig. 1. Activity-dependent labeling and light-activation of hippocampal neurons, and the basic experimental scheme. (A) The *c-fos-tTA* mice were bilaterally injected with AAV, TRE-ChR2-mCherry and implanted with optical fibers targeting DG. **(B)** While on Dox, exploration of a novel context did not induce expression of ChR2-mCherry. **(C)** While off Dox, exploration of a novel context induced expression of ChR2-mCherry in DG. **(D)** Light pulses induced spikes in a CA1 neuron expressing ChR2-mCherry. The recorded neuron is shown labeled with biocytin in **(E)**. **(F)** Light pulses induced spikes in DG neurons recorded from a head-fixed anesthetized *c-fos-tTA* animal expressing ChR2-mCherry. **(G)** Basic experimental scheme. Post-surgery mice were taken off Dox and allowed to explore context A in order to let DG or CA1 cells become labeled with ChR2-mCherry. Mice were put back on Dox and fear conditioned in context B with simultaneous delivery of light pulses. Freezing levels were then measured in both the original context A and a novel context C. The light green shading indicates the presence of Dox in the diet during corresponding stages of the scheme. Prime indicates the second exposure to a given context. The yellow lightning symbol and blue shower symbol indicate foot shocks and blue light delivery, respectively. Red circles represent neurons encoding context A that are thus labeled with ChR2-mCherry. Gray and white circles represent neurons encoding context B and C, respectively. Asterisks indicate neurons activated either by exposure to context or light stimulation.



(EYFP) instead of ChR2-mCherry in the DG that underwent the same behavioral schedule also showed increased freezing in context A (fig. S2A).

New experimental and control groups of mice were taken off Dox in context A in order to label activated cells and then placed in context C on the following day while back on Dox. In this experiment, although conditioning took place after the formation of both context A and context C memories, only those cells encoding context A were reactivated by light during fear conditioning. Subsequently, all groups of mice displayed background levels of freezing in context C. In contrast, in the context A test the next day, the experimental group showed increased freezing levels as compared with those of the mCherry-only group, confirming that the recall of the false memory is specific to context A (Fig. 2G). This freezing was not observed in another ChR2-mCherry group that underwent the same behavioral protocol but without light stimulation during fear conditioning in context B, or in a group in which an immediate shock protocol was administered in context B with light stimulation of context A cells (Fig. 2G and fig. S3). In a separate group of animals, we labeled cells active in context C rather than context A and repeated similar

experiments as above. These animals showed freezing in context C but not context A (fig. S2B).

The hippocampus processes mnemonic information by altering the combined activity of subsets of cells within defined subregions in response to discrete episodes (11–13). Therefore, we investigated whether applying the same parameters and manipulations to CA1 as we did to the DG could form a false memory. We first confirmed that light could activate cells expressing ChR2-mCherry along the anterior-posterior axis of the CA1 similar to the DG (fig. S1, J to R). Also similar to the DG (Fig. 2, A to E), the overlap of active CA1 cells was significantly lower across contexts (A and C) as compared with that of a reexposure to the same context (A and A). However, the degree of overlap for the two contexts was much greater in CA1 (30%) than in the DG (~1%). When we labeled CA1 cells activated in context A and reactivated these cells with light during fear conditioning in context B, no increase in freezing was observed in the experimental group expressing ChR2-mCherry as compared with the mCherry-only control group in either context A or context C, regardless of whether the animals were exposed to context C or not before fear conditioning in context B (Fig. 2, M and N).

The simultaneous availability of two CSs can sometimes result in competitive conditioning; the memory for each individual CS is acquired less strongly as compared with when it is presented alone, and the presentation of two simultaneous CSs to animals trained with a single CS can also lead to decrement in recall (14). In our experiments, it is possible that the light-activated DG cells encoding context A interfered with the acquisition or expression of the genuine fear memory for context B. Indeed, upon reexposure to context B, the experimental group froze significantly less than the group that did not receive light during fear conditioning or the group expressing mCherry alone (Fig. 3A and fig. S4). During light-on epochs in the context B test, freezing increased in the experimental group and decreased in the group that did not receive light during fear conditioning (Fig. 3A and fig. S2C). We conducted similar experiments with mice in which the manipulation was targeted to the CA1 region and found no differences in the experimental or control groups during either light-off or light-on epochs of the context B test (fig. S5A).

Memory recall can be induced for a genuine fear memory by light reactivation of the corresponding engram in the DG (8). To investigate

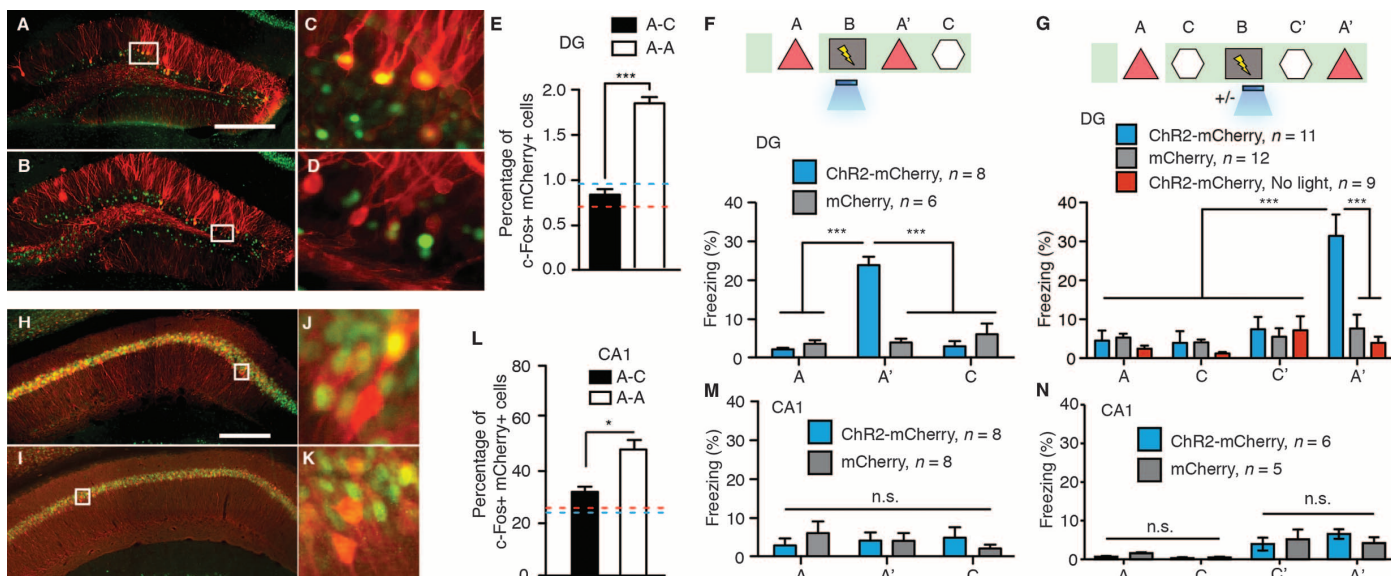


Fig. 2. Creation of a false contextual fear memory. (A to E) c-fos-TIA mice injected with AAV₉-TRE-ChR2-mCherry in the DG were taken off Dox and exposed to context A in order to label the activated cells with mCherry (red), then put back on Dox and exposed to the same context A [(A) and (C)] or a novel context C [(B) and (D)] 24 hours later so as to let activated cells express c-Fos (green). Images of the DG from these animals are shown in (A) to (D), and the quantifications are shown in (E) ($n = 4$ subjects each; *** $P < 0.001$, unpaired Student's t test). Blue and red dashed lines indicate the chance level of overlap for A-A and A-C groups, respectively. (F) (Top) Training and testing scheme of animals injected with AAV₉-TRE-ChR2-mCherry or AAV₉-TRE-mCherry. Various symbols are as explained in Fig. 1. (Bottom) Animals' freezing levels in context A before fear conditioning and in context A and C after fear conditioning [$n = 8$ subjects for ChR2-mCherry group, and $n = 6$ subjects for mCherry group; *** $P < 0.001$, two-way analysis of variance (ANOVA) with repeated measures followed by Bonferroni post-hoc test]. (G) (Top) Training and testing scheme of animals injected with AAV₉-TRE-ChR2-

mCherry or AAV₉-TRE-mCherry. One control group injected with AAV₉-TRE-ChR2-mCherry did not receive light stimulation during fear conditioning (ChR2-mCherry, no light). (Bottom) Animals' freezing levels in context A and C before and after fear conditioning ($n = 11$ subjects for ChR2-mCherry group, $n = 12$ subjects for mCherry, and $n = 9$ subjects for ChR2-mCherry, no-light groups; *** $P < 0.001$, two-way ANOVA with repeated measures followed by Bonferroni post-hoc test). (H to L) Animals underwent the same protocol as in (A) to (E), except the virus injection was targeted to CA1. Representative images of CA1 from these animals are shown in (H) to (K), and the quantifications are shown in (L) ($n = 4$ subjects each; * $P = 0.009$, unpaired Student's t test). (M) Same as (F), except the viral injection and implants were targeted to CA1 ($n = 8$ subjects for ChR2-mCherry and mCherry groups; n.s., not significant; two-way ANOVA with repeated measures followed by Bonferroni post-hoc test). (N) Same as (G), except the viral injection and implants were targeted to CA1 ($n = 6$ subjects for ChR2-mCherry group and $n = 5$ subjects for mCherry group). Scale bar in (A) and (H), 250 μ m.

whether this applies to a false fear memory, we examined fear-memory recall of experimental and control groups of mice in a distinct context (context D) with light-off and light-on epochs (Fig. 3B). All groups exhibited background levels of freezing during light-off epochs. The experimental group, however, froze at significantly higher levels (~25%) during light-on epochs. This light-induced freezing in context D was not observed in control animals that underwent the same behavioral schedule but did not receive light during fear conditioning in context B, in animals expressing mCherry alone, in animals receiving immediate shock, or in animals in which CA1 was manipulated instead (Fig. 3B and figs. S2D, S3C, S4C, and S5B).

Moreover, we quantified the levels of c-Fos expression in the basolateral amygdala (BLA) and the central amygdala (CeA) during the recall of a false and genuine fear memory (15–20). Both sessions elicited a significant increase in c-Fos-positive cells in the BLA and CeA compared with a control group exploring a neutral context (Fig. 3, C to F).

Last, a new cohort of mice was trained in a conditioned place avoidance (CPA) paradigm (21). Naïve animals did not show an innate preference for either chamber across multiple days (fig. S6A). An experimental group injected with the ChR2-mCherry virus and a control group injected with the mCherry-only virus were taken off Dox and exposed to one chamber of the CPA apparatus in order to label the DG cells activated in this chamber. These animals were then placed back on Dox and on the following day were exposed to the opposite chamber. Next, the mice were fear conditioned in a different context with light stimulation. The following day, they were placed back into the CPA apparatus, and their preference between the chambers was measured (Fig. 4A). After conditioning, the experimental group showed a strong preference for the unlabeled chamber over the labeled chamber, whereas the mCherry-only group spent an equal amount of time exploring both chambers (Fig. 4, B to D, and fig. S6B). Exposure to the two chambers activated a statistically independent population of DG cells (Fig. 4, E to K). We conducted similar behavioral tests targeting the CA1 subregion of the hippocampus, and the experimental group did not show any chamber preference (Fig. 4, L and M).

Our results show that cells activated previously in the hippocampal DG region can subsequently serve as a functional CS in a fear-conditioning paradigm when artificially reactivated during the delivery of a unconditioned stimulus (US). The consequence is the formation of a false associative fear memory to the CS that was not naturally available at the time of the US delivery. This is consistent with previous findings that high-frequency stimulation of the perforant path, an input to DG, can serve as a CS in a conditioned suppression paradigm (22).

Memory is constructive in nature; the act of recalling a memory renders it labile and highly

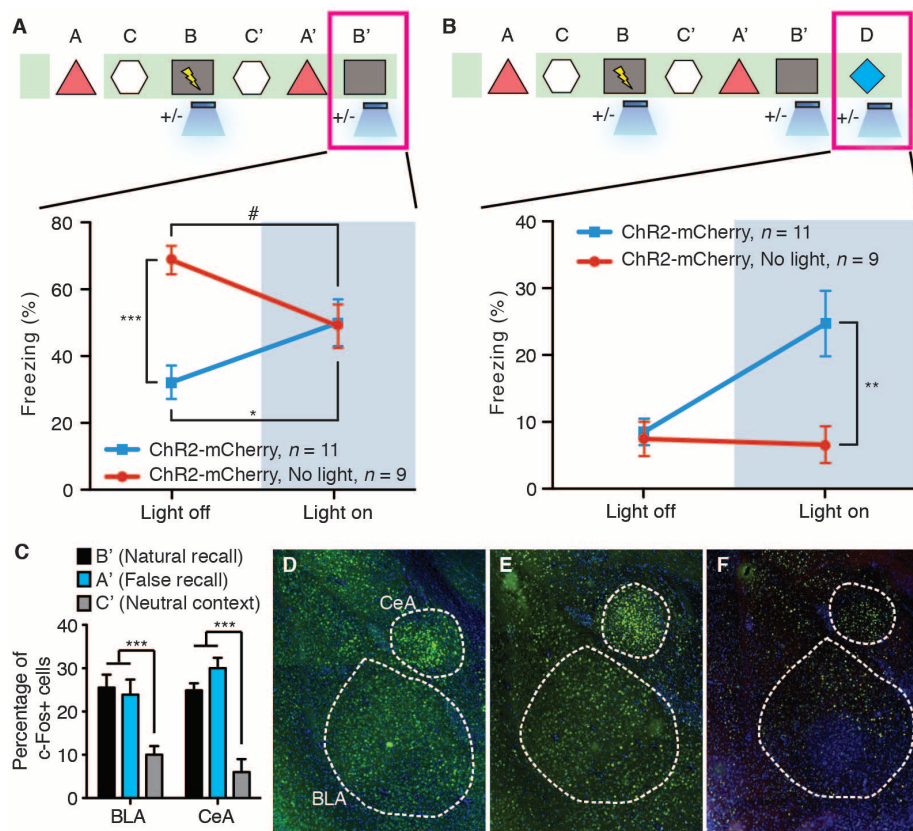


Fig. 3. The false and genuine fear memories interact with each other, and both recruit the amygdala. (A) Animals that underwent the behavioral protocol shown in Fig. 2G were reexposed to context B, and the freezing levels were examined both in the absence and presence of light stimulation ($n = 11$ subjects for ChR2-mCherry group and $n = 9$ subjects for ChR2-mCherry, no-light group; $*P = 0.027$; $***P < 0.001$; $\#P = 0.034$, two-way ANOVA with repeated measures followed by Bonferroni post-hoc test). (B) Animals that underwent the behavioral protocol shown in (A) were placed in a novel context D, and the freezing levels were examined both in the absence and presence of light stimulation ($n = 11$ subjects for ChR2-mCherry group and $n = 9$ subjects for ChR2-mCherry, no-light group; $**P = 0.007$, two-way ANOVA with repeated measures followed by Bonferroni post-hoc test). (C) Three groups of mice underwent the training shown in (A) and were euthanized after testing in either context B (natural recall), A (false recall), or C (neutral context). The percentage of c-Fos-positive cells was calculated for each group in basolateral amygdala (BLA) and central amygdala (CeA) ($n = 6$ subjects each; $***P < 0.001$). (D to F) Images for natural recall, false recall, or neutral context.

susceptible to modification (23, 24). In humans, memory distortions and illusions occur frequently. These phenomena often result from the incorporation of misinformation into memory from external sources (25–27). Cognitive studies in humans have reported robust activity in the hippocampus during the recall of both false and genuine memories (28). However, human studies performed using behavioral and functional magnetic resonance imaging techniques have not been able to delineate the hippocampal subregions and circuits that are responsible for the generated false memories. Our experiments provide an animal model in which false and genuine memories can be investigated at the memory-gram level (29). We propose that optical reactivation of cells that were naturally activated during the formation of a contextual memory induced the retrieval of that memory, and the retrieved memory became associated with an event of high valence (a foot shock) to form a new but false memory. Thus, the

experimental group of animals showed increased freezing in a context in which they were never shocked (context A). Although our design for the formation and expression of a false memory was for a laboratory setting, and the retrieval of the contextual memory during conditioning occurred by artificial means (light), we speculate that the formation of at least some false memories in humans may occur in natural settings through the internally driven retrieval of a previously formed memory and its association with concurrent external stimuli of high valence.

Our experiments also allowed us to examine the dynamic interaction between the false and genuine memories at different stages of the memory process. During the acquisition phase, the artificial contextual information (context A by light activation) either competed with the genuine contextual cues (context B by natural exposure) for the valence of the US (foot shock), or may have interfered with the perception of the genuine

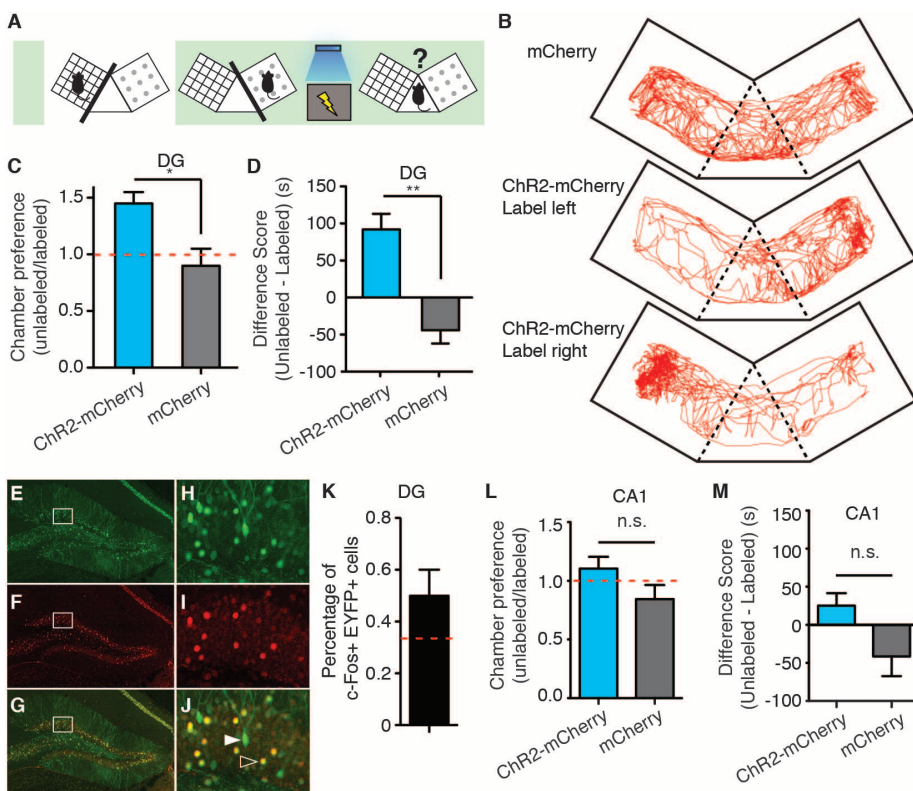


Fig. 4. The false memory supports active fear behavior. (A) The scheme for conditioned place avoidance paradigm. Various symbols are as explained in Fig. 1. (B) Locomotion traces during testing from animals injected with AAV₉-TRE-mCherry (top), or animals injected with AAV₉-TRE-ChR2-mCherry and DG cells subsequently labeled, corresponding to either the left (middle) or right (bottom) chamber. (C and D) ChR2-mCherry and mCherry group preferences for the labeled versus unlabeled chambers as shown by the ratio (C) or the difference in duration of the time spent in each chamber (D). ($n = 8$ subjects; * $P = 0.013$; ** $P = 0.008$, unpaired Student's t test). The red dashed line indicates no preference. (E to K), c-fos-tTA mice injected with AAV₉-TRE-EYFP in the DG were taken off Dox and exposed to one chamber in order to label the activated cells with EYFP (green) then put back on Dox and exposed to the opposite chamber 24 hours later to let activated cells express c-Fos (red). Expression of EYFP [(E) and (H)], expression of c-Fos [(F) and (I)], and a merged view [(G) and (J)] are shown. Solid arrows indicate cells expressing EYFP. Open arrows indicate cells expressing c-Fos. These cells appear yellow because they express both endogenous c-Fos (red) and the nuclear-localized c-fos-shEGFP (green) from the mouse line (10). Quantifications from the dorsal blades of the DG are shown in (K) ($n = 4$ subjects). Red dashed lines indicate the chance level of overlap. (L and M) Same as (C) and (D), except the viral injection and implants were targeted to CA1 ($n = 6$ subjects each group).

contextual cues. This resulted in reduced expression of both false and genuine fear memories compared with the strength of recall attainable after normal fear conditioning (Fig. 3A, the two groups during the light-off epoch). This could also be related to the overshadowing effects for multiple CSs (30). During the recall phase in context B, the false memory and the genuine memory were either additive (Fig. 3A, the with-light group during light-off and light-on epochs) or competitive (Fig. 3A, the no light group during light-off and light-on epochs). All of these observations are consistent with the predictions of an updated Rescorla-Wagner componential model for two independent CSs and suggest that the light-activated artificial CS is qualitatively similar to the genuine CS (14).

A previous study applied a similar experimental protocol with pharmacosynthetic methods and failed to see increased freezing upon reexposure

to either context A or context B. Instead, they observed a synthetic memory that could only be retrieved by the combination of both contexts A and B (9). A key difference in their system is that the c-Fos-expressing cells in the entire forebrain were labeled and reactivated over an extended period by a synthetic ligand. We propose that activating neurons in much wider spatial and temporal domains may favor the formation of a synthetic memory, which may not be easily retrievable by the cues associated with each individual memory. In contrast, activating neurons in a more spatially (only small populations of DG cells) and temporally restricted manner (only a few minutes during light stimulation) may favor the formation of two distinct (false and genuine) memories as observed in our case. In line with this hypothesis, when we manipulated CA1 cells by the same procedures as the ones used for DG cells, we could not create a false memory (freez-

ing in context A). In CA1, the overlap of the cell populations activated by consecutive exposures to a pair of contexts is much greater than in the DG. Although additional work is needed to reveal the nature of CA1 engrams, we hypothesize that our negative CA1 behavioral data could be a result of contextual engrams relying less on a population code and increasingly on a temporal code as they travel through the trisynaptic circuit (4, 11–13).

References and Notes

1. D. L. Schacter, D. R. Addis, R. L. Buckner, *Nat. Rev. Neurosci.* **8**, 657–661 (2007).
2. E. Pastalkova, V. Itskov, A. Amarasingham, G. Buzsaki, *Science* **321**, 1322–1327 (2008).
3. H. Gelbard-Sagiv, R. Mukamel, M. Harel, R. Malach, I. Fried, *Science* **322**, 96–101 (2008).
4. C. J. MacDonald, K. Q. Lepage, U. T. Eden, H. Eichenbaum, *Neuron* **71**, 737–749 (2011).
5. G. Buzsaki, E. I. Moser, *Nat. Neurosci.* **16**, 130–138 (2013).
6. T. J. McHugh *et al.*, *Science* **317**, 94–99 (2007).
7. D. Tse *et al.*, *Science* **316**, 76–82 (2007).
8. X. Liu *et al.*, *Nature* **484**, 381–385 (2012).
9. A. R. Garner *et al.*, *Science* **335**, 1513–1516 (2012).
10. L. G. Reijmers, B. L. Perkins, N. Matsuo, M. Mayford, *Science* **317**, 1230–1233 (2007).
11. S. Kubik, T. Miyashita, J. F. Guzowski, *Learn. Mem.* **14**, 758–770 (2007).
12. J. F. Guzowski, B. L. McNaughton, C. A. Barnes, P. F. Worley, *Nat. Neurosci.* **2**, 1120–1124 (1999).
13. J. K. Leutgeb, S. Leutgeb, M. B. Moser, E. I. Moser, *Science* **315**, 961–966 (2007).
14. S. E. Brandon, E. H. Vogel, A. R. Wagner, *Behav. Brain Res.* **110**, 67–72 (2000).
15. J. H. Han *et al.*, *Science* **323**, 1492–1496 (2009).
16. M. T. Rogan, U. V. Stäubli, J. E. LeDoux, *Nature* **390**, 604–607 (1997).
17. J. P. Johansen *et al.*, *Proc. Natl. Acad. Sci. U.S.A.* **107**, 12692–12697 (2010).
18. S. Maren, G. J. Quirk, *Nat. Rev. Neurosci.* **5**, 844–852 (2004).
19. H. Li *et al.*, *Nat. Neurosci.* **16**, 332–339 (2013).
20. S. Ciocchi *et al.*, *Nature* **468**, 277–282 (2010).
21. S. Lammel *et al.*, *Nature* **491**, 212–217 (2012).
22. V. Doyère, S. Laroche, *Hippocampus* **2**, 39–48 (1992).
23. K. Nader, G. E. Schafe, J. E. Le Doux, *Nature* **406**, 722–726 (2000).
24. F. C. Bartlett, *Remembering: A Study in Experimental and Social Psychology* (Cambridge Univ. Press, Cambridge, 1932).
25. E. F. Loftus, *Nat. Rev. Neurosci.* **4**, 231–234 (2003).
26. D. L. Schacter, E. F. Loftus, *Nat. Neurosci.* **16**, 119–123 (2013).
27. H. L. Roediger, K. B. McDermott, *J. Exp. Psychol. Learn. Mem. Cogn.* **24**, 803–814 (1995).
28. R. Cabeza, S. M. Rao, A. D. Wagner, A. R. Mayer, D. L. Schacter, *Proc. Natl. Acad. Sci. U.S.A.* **98**, 4805–4810 (2001).
29. S. M. McTighe, R. A. Cowell, B. D. Winters, T. J. Bussey, L. M. Saksida, *Science* **330**, 1408–1410 (2010).
30. I. P. Pavlov, *Conditioned Reflexes* (Oxford University Press, Oxford, 1927).

Acknowledgments: We thank S. Huang, M. Serock, A. Mockett, J. Zhou, and D. S. Roy for help with the experiments; J. Z. Young and K. L. Mulroy for comments and discussions on the manuscript; and all the members of the Tonegawa lab for their support. This work was supported by the RIKEN Brain Science Institute.

Supplementary Materials

www.sciencemag.org/cgi/content/full/341/6144/387/DC1
Materials and Methods
Figs. S1 to S6
References

12 April 2013; accepted 2 July 2013
10.1126/science.1239073

Creating a False Memory in the Hippocampus

Steve Ramirez, Xu Liu, Pei-Ann Lin, Junghyup Suh, Michele Pignatelli, Roger L. Redondo, Tomás J. Ryan and Susumu Tonegawa

Science 341 (6144), 387-391.
DOI: 10.1126/science.1239073

Can You Trust Your Memory?

Being highly imaginative animals, humans constantly recall past experiences. These internally generated stimuli sometimes get associated with concurrent external stimuli, which can lead to the formation of false memories. **Ramirez et al.** (p. 387; see the cover) identified a population of cells in the dentate gyrus of the mouse hippocampus that encoded a particular context and were able to generate a false memory and study its neural and behavioral interactions with true memories. Optogenetic reactivation of memory engram-bearing cells was not only sufficient for the behavioral recall of that memory, but could also serve as a conditioned stimulus for the formation of an associative memory.

ARTICLE TOOLS

<http://science.scienmag.org/content/341/6144/387>

SUPPLEMENTARY MATERIALS

<http://science.scienmag.org/content/suppl/2013/07/25/341.6144.387.DC2>
<http://science.scienmag.org/content/suppl/2013/07/24/341.6144.387.DC1>

RELATED CONTENT

<http://science.scienmag.org/content/sci/341/6144/415.2.full>

REFERENCES

This article cites 28 articles, 12 of which you can access for free
<http://science.scienmag.org/content/341/6144/387#BIBL>

PERMISSIONS

<http://www.scienmag.org/help/reprints-and-permissions>

Use of this article is subject to the [Terms of Service](#)

Science (print ISSN 0036-8075; online ISSN 1095-9203) is published by the American Association for the Advancement of Science, 1200 New York Avenue NW, Washington, DC 20005. The title *Science* is a registered trademark of AAAS.

Copyright © 2013, American Association for the Advancement of Science

Supplementary Material for **Creating a False Memory in the Hippocampus**

Steve Ramirez, Xu Liu, Pei-Ann Lin, Junghyup Suh, Michele Pignatelli, Roger L. Redondo, Tomás J. Ryan, Susumu Tonegawa*

*Corresponding author. E-mail: tonegawa@mit.edu

Published 26 July 2013, *Science* **341**, 387 (2013)
DOI: 10.1126/science.1239073

This PDF file includes:

Materials and Methods

Figs. S1 to S6

References

Materials and methods

Subjects

The c-fos-tTA mice were generated by crossing TetTag (*S1*) mice with C57BL/6J mice and selecting those carrying the *c-fos-tTA* transgene. Mice were group-housed with littermates until the beginning of the surgery and given food and water *ad libitum*. The mice were 8–14 weeks old at the time of surgery and had been raised on a diet containing 40 mg kg⁻¹ doxycycline for a minimum of 1 week before surgery. Mice were housed individually post-surgery and throughout the duration of the experiments. All procedures relating to mouse care and treatment conformed to the institutional and National Institutes of Health guidelines.

Virus constructs

The pAAV-TRE-ChR2-mCherry plasmid was constructed by replacing the *EYFP* sequence in the pAAV-TRE-ChR2-EYFP plasmid (*S2*) with the sequence for *mCherry* using *AgeI* and *BsrGI* restriction sites. The pAAV-TRE-mCherry plasmid was constructed by removing the *ChR2* fragment from the pAAV-TRE-ChR2-mCherry plasmid using *NheI* and *AgeI* restriction sites, blunting with T4 DNA polymerase, and self-ligating the vector, which retained the ATG start codon of the *mCherry* gene from the *ChR2-mCherry* fusion gene. These plasmids were used to generate AAV₉ viruses by the Gene Therapy Center and Vector Core at the University of Massachusetts Medical School. Viral titers were 8×10^{12} GC/ml for AAV₉-TRE-ChR2-mCherry and 1.4×10^{13} GC/ml for AAV₉-TRE-mCherry. Viral titers were 1×10^{13} GC/ml for AAV₉-TRE-ChR2-EYFP and 1.5×10^{13} GC/ml for AAV₉-TRE-EYFP as previously reported (*S2*).

Stereotactic injection and optical fiber implant

All surgeries were performed under stereotaxic guidance. Mice were anaesthetized using 500 mg kg⁻¹ Avertin. Each animal underwent bilateral craniotomies using a 0.5 mm diameter drill bit at -2.2 mm anterioposterior (AP), ± 1.3 mm mediolateral (ML) for DG injections; -2.0 mm AP, ± 1.5 mm ML for CA1

injections (S3). The virus was injected using a mineral oil-filled glass micropipette joined by a microelectrode holder to a 10 μ l Hamilton microsyringe. A microsyringe pump and its controller were used to control the speed of the injection. The needle was slowly lowered to the target site (-2.0 mm dorsoventral (DV) for DG injections; -1.2 mm DV for CA1 injections) and remained for five min before the beginning of the injection. All mice were injected bilaterally with 0.15 μ l AAV₉ virus at a rate of 0.6 μ l min⁻¹. The micropipette was kept at the target site for another five minutes post-injection before being slowly withdrawn. After withdrawing of the needle, a bilateral patch cord optical fiber implant (200 μ m core diameter) was lowered above the injection site (-1.6 mm DV for DG; -1.0 mm DV for CA1). A miniature screw was screwed securely into the skull at the anterior and posterior edges of the surgical site to provide two extra anchor points for the implant. A layer of adhesive cement was applied to secure the optical fiber implant to the skull. A protective cap made from the top portion of a black polypropylene microcentrifuge tube was used to encircle the surgical site, and dental cement was applied to secure the cap to the implant and close up the surgical site. Each animal was given 1.5 mg kg⁻¹ analgesics via intraperitoneal injection and remained on a heating pad until fully recovered from anesthesia. All mice were allowed to recover for two weeks before all subsequent experiments. All fiber placements and viral injection sites were verified histologically. We only included mice in this study that had opsin or fluorophore expression limited to either DG or to CA1.

Slice recordings

Mice (P30–P35) were anesthetized by isoflurane, decapitated and brains were quickly removed. Sagittal slices (300 μ m thick) were prepared by using a vibratome in an oxygenated cutting solution at ~4 °C. Slices were then incubated at room temperature (~23 °C) in oxygenated ACSF until the recordings. The cutting solution contained (in mM): 3 KCl, 0.5 CaCl₂, 10 MgCl₂, 25 NaHCO₃, 1.2 NaH₂PO₄, 10 D-glucose, 230 sucrose, saturated with 95% O₂ – 5% CO₂ (pH 7.3, osmolarity 300 mOsm). The ACSF contained (in mM): 124 NaCl, 3 KCl, 2 CaCl₂, 1.3 MgSO₄, 25

NaHCO₃, 1.2 NaH₂PO₄, 10 D-glucose, saturated with 95% O₂ – 5% CO₂ (pH 7.3, osmolarity 300 mOsm). Individual slices were transferred into a submerged experimental chamber and perfused with oxygenated ACSF warmed at 36 °C (± 0.5 °C) at a rate of 3 ml/min during recordings. Whole cell recordings in current clamp or voltage clamp mode were performed by using an IR-DIC microscope mounting a water immersion 40× objective (NA 0.8), equipped with four automatic manipulators and a CCD camera. For all the recordings borosilicate glass pipettes were fabricated with resistances of 8 to 10 MΩ, and filled with the following intracellular solution (in mM): 110 K-gluconate, 10 KCl, 10 HEPES, 4 ATP, 0.3 GTP, 10 phosphocreatine and 0.5% biocytin. The osmolarity of this intracellular solution was 290 mOsm and the pH was 7.25. Access resistance (Ra) was monitored throughout the duration of the experiment and data acquisition was suspended whenever the resting membrane potential was depolarized above -50 mV or the Ra was beyond 20 MΩ. Recordings were amplified using up to two dual channel amplifiers, filtered at 2 kHz, digitized (20 kHz), and acquired using custom made software running on Igor Pro. Optogenetic stimulation was achieved through a 460 nm LED light source driven by TTL input with a delay onset of 25 µs (subtracted off-line for the estimation of the latencies). Light power on the sample was 33 mW/mm². Slices were stimulated by a train of twenty 15 ms light pulses at 20 Hz every 5 s. In voltage clamp mode cells were held at -70 mV for EPSC measurements while in current clamp mode, EPSP and APs were measured at resting potentials.

Head-fixed recording

Mice were anaesthetized by injection (100 ml kg⁻¹) of a mixture of ketamine (100 mg ml⁻¹) / xylazine (20 mg ml⁻¹) and placed in the stereotactic instrument with anaesthesia maintained with a series of ketamine boost (100 mg ml⁻¹) throughout the recording. Body temperature was maintained by a pack of Hand Warmers. An optrode consisting of a tungsten electrode (0.5 MΩ) attached to an optical fiber (200 µm core diameter), with the tip of the electrode extending beyond the tip of the fiber by 300 µm, was used for simultaneous optical stimulation and

extracellular recordings. The optrode was slowly lowered to the DG (AP -2.2 mm; ML +1.3 mm; DV -2.0 mm) using a hydraulic micropositioner at a speed of 50 μ m per 5–10 min. The optical fiber was connected to a 200 mW 473 nm blue laser and controlled by a waveform generator. The power intensity of light emitted from the optrode was calibrated to about 7 mW, which was consistent with the power intensity used in the behavioral assays. To identify ChR2-labelled cells, light pulses of 15 ms were delivered at 0.2 Hz at the recording sites approximately every 50 μ m throughout the DG. After light responsive cells were detected, two types of light stimuli were tested: 15 ms light pulse every 5 s and a train of ten 15 ms light pulses at 20 Hz every 5 s. Unit activity was band-pass filtered (500 Hz–5 kHz) and acquired with an Axon Digidata 1440A acquisition system running Clampex 10.2 software. Data were analyzed with custom software written in Matlab. After the recording, endogenous c-Fos expression was induced by delivering two epochs of 3-min light stimulation (7 mW, 20 Hz, 15 ms), separated by 3 min, to the DG, the same as in behavioral experiments (see below). Mice were sacrificed and perfused 90 min later.

Immunohistochemistry

Mice were overdosed with 750–1000 mg kg⁻¹ Avertin and perfused transcardially with cold PBS, followed by 4% paraformaldehyde (PFA) in PBS. Brains were extracted from the skulls and kept in 4% PFA at 4 °C overnight, then transferred to PBS. Fifty μ m coronal slices were taken using a vibratome and collected in cold PBS. For immunostaining, each slice was placed in PBS-T (PBS + 0.2% Triton X-100) with 5% normal goat serum for 1 h and then incubated with one or more primary antibodies (1:1000 dilution) at 4°C for 24 h (600-401-379 Rockland; A10262, Invitrogen; SC-52, Santa Cruz). Slices then underwent three wash steps for 10 min each in PBS-T, followed by 1 h incubation with secondary antibody at 1:200 dilution (A11039, Invitrogen; A21429, Invitrogen). Slices then underwent three more wash steps of 10 min each in PBS-T, including DAPI (1:10000 dilution) in the first wash step, followed by mounting with Vectashield H-1200 and coverslipping on microscope slides.

Behavior assays

All behavior tests were administered during the light cycle (7 am –7 pm) of the day. Contextual fear conditioning assays were conducted in one of the four distinct contexts (A, B, C, and D). Context A was a 29 × 25 × 22 cm chamber with removable black cardboard floor and scented with 1% acetic acid from a tray underneath. Within each chamber was a black plastic triangular roof. Context A was located underneath two lamps emitting red light in a room with dim lighting. Context B was a 30 × 25 × 33 cm chamber with metal gridded floor and scented with 0.25% benzaldehyde. It is located in a second room with black walls, black curtains, and intermediate lighting. Context C was a 29 × 25 × 22 cm chamber with glossy white plastic floor and scented with 1 ml of citral in a tray underneath the floor. It is in a third room with bright light distinct from context A and B. Context D was a 32 × 25 × 27 cm unscented chamber with matte white plastic floor within a 64 × 73 × 40 sound attenuating cubicle with internal lightings. It is located in a fourth room distinct from contexts A, B, and C.

Prior to the behavioral experiments, all mice were handled for five days. They were taken off Dox for 42 hours to open a window of activity-dependent labeling. They were then placed in context A and allowed to explore for ten minutes, after which they were immediately removed from the chamber and placed on 40 mg kg⁻¹ Dox diet to shut off further labeling. Twenty-four hours later, mice were individually placed into context B and plugged to a complimentary optical fiber patch cord, which was connected to a 473 nm laser under the control of a function generator. Mice were trained in context B for a total of 420 s. They were first allowed to explore context B for 120 s, after which blue light was administered (20 Hz, 15 ms pulse width, ~7–15 mW output from fiber tip) for the remaining 300 seconds. At 240 s into training, three mild foot shocks (0.75 mA) lasting 2 seconds each were administered with a sixty-second inter-shock interval. At the 420 s mark, mice were immediately removed from context B and placed back into their home cages. All post-training tests in contexts A (A') and C (C') consisted of three-minute exposure to the contexts. Test trials during re-exposure to context B (B') or

exposure to context D each lasted six minutes, beginning with a three-minute light-off epoch followed by a three-minute light-on epoch, with the same light stimulation parameters as the training session. Separate cohorts of mice underwent a similar behavioral schedule but were pre-exposed to context C for 10 min while on Dox a day after the first exposure to context A (Fig. 2G, N). The immediate shock group underwent the same behavioral protocol described for the group in which context A was labeled, except that training in context B lasted for 10 s with light stimulation, at the end of which a single 0.75 mA shock was administered for 2 s. While mice were in contexts A and C, freezing behavior was continuously recorded with a digital camera and measured with FreezeFrame software. Light stimulation during training on context B, re-exposure to context B (B'), or exposure to context D interfered with the motion detection of the program. To circumvent this issue, freezing during these sessions was manually scored by two experimenters in a double-blind fashion. The manual scoring and automated scoring yielded freezing scores with a difference of less than 5%.

For the conditioned place avoidance (CPA) experiments, the CPA apparatus consisted of two $15 \times 15 \times 20$ cm chambers (A and B) connected by a triangular neutral zone (15 cm for each side). Chamber A consisted of black and white striped walls and contained a transparent floor with small irregular indentations. Chamber B consisted of black and white alternating polka dotted walls and contained a smooth plastic floor. The mice did not have an innate preference for either portion of the apparatus (fig. S6A). Experimental mice were first taken off Dox for 42 hours to open a window of activity-dependent labeling. They were then exposed in a counterbalanced manner to either chamber A or B (labeled chamber) for ten minutes to label the cells active in the respective chamber. Then they were placed back on Dox diet and exposed to the other chamber (unlabeled chamber) 24 h later. These mice then underwent the same fear conditioning protocol with light stimulation in context B as described above. Twenty-four hours later, all groups were placed in the neutral zone of the CPA apparatus and preference scores were measured continuously across a twelve-minute session by automated scoring software. To calculate preference scores, we divided the total amount of time that

each animal spent in the unlabeled chamber by the total amount of time it spent in the labeled chamber. Thus a value above 1 indicates a preference for the unlabeled chamber; and a value below 1 indicates a preference for the labeled chamber. Moreover, to calculate difference scores, we subtracted the total amount of time each animal spent in the unlabeled chamber by the total amount of time the animal spent in the labeled chamber.

Cell counting

To measure the extent to which populations of active cells overlap between the exposure to the same or different contexts, we counted the number of mCherry and c-Fos immunoreactive neurons in DG and CA1 from five coronal slices (spaced 160 μm from each other) per mouse ($n = 4$ for all groups). These slices were taken from dorsal hippocampus and focused on the coordinates that our injection and optical fiber implants targeted (-1.94 mm to -2.74 mm AP). Fluorescence images were acquired using a microscope with a $\times 20/0.50 \text{ NA}$ objective. Mice injected with AAV-TRE-ChR2-mCherry in DG and CA1 were first taken off Dox for 42 hours to open a period of activity-dependent labeling. They were then placed in context A for ten minutes to label the cells active in this environment and placed on Dox immediately following the session. The next day, half of the mice were placed back in context A (the A-A group) and half were placed in a distinct context C (the A-C group). Both groups were sacrificed 1.5 h later for immunohistochemistry analyses. The overlap between mCherry and c-Fos in these experiments was quantified with ImageJ (S4). Background autofluorescence was removed by applying an equal cutoff threshold to all images by an experimenter blind to experimental conditions. Statistical chance was calculated by multiplying the observed percentage of mCherry-single-positive cells by the observed percentage of c-Fos-single-positive-cells.

To measure the extent to which false and genuine memories engage similar brain regions, mice were taken off Dox for 42 hours and then exposed to context A for ten minutes to label DG cells with ChR2-mCherry. The following day, they were

exposed to context C while on Dox for ten minutes. These mice were then divided into three groups: two groups underwent fear conditioning in context B with light stimulation as described above, and one group with no light stimulation during fear conditioning. For the first two groups, one group was then re-exposed to context C (C') and sacrificed 1.5 h later. The other group was re-exposed to context A (A') for a false memory test and sacrificed 1.5 h later. The third group, which did not receive light during fear conditioning, was re-exposed to context B (B') for natural fear memory recall, and sacrificed 1.5 h later.

Automated cell counting of c-Fos-positive cells was performed in the amygdala by utilizing image analysis software. This module quantified the number of c-Fos-positive cells per section (5 coronal slices per mouse; $n = 6$ mice per condition) by thresholding c-Fos immunoreactivity above background levels and by using DAPI staining to differentiate between nuclei. Our regions of interest (ROI) included the basolateral amygdala and central amygdala. Our sampled amygdala slices were spaced at least 40 μm from each other and we focused on slices between -1.30 mm to -1.70 mm from Bregma. Each ROI was manually outlined for quantification. For statistical analysis, we used a one-way ANOVA followed by Tukey's multiple comparisons ($\alpha = 0.05$). All data were analyzed and graphed using Microsoft Excel with the Statplus plug-in and Prism.

In a separate group of c-fos-tTA animals injected with AAV₉-TRE-ChR2-mCherry targeted to either the DG or CA1, we determined the extent to which light activates cells along the anterior-posterior axis of these subregions. These groups were taken off Dox and exposed to context A for 10 min to induce ChR2-mCherry in DG or CA1. While back on Dox, light stimulation was administered (300 sec, ~9 mW, 20 Hz, 15 ms pulse width) the following day in context D and animals were sacrificed 1.5 hours later for histological analyses and quantification of cFos-positive cells using the immunohistochemistry protocol described above. The intermediate slices were defined as slices directly underneath the center of our optic fiber implant (-2.2 mm AP for DG and -2.0 mm AP for CA1) whereas anterior or posterior slices were selected 500 μm away from the intermediate slices.

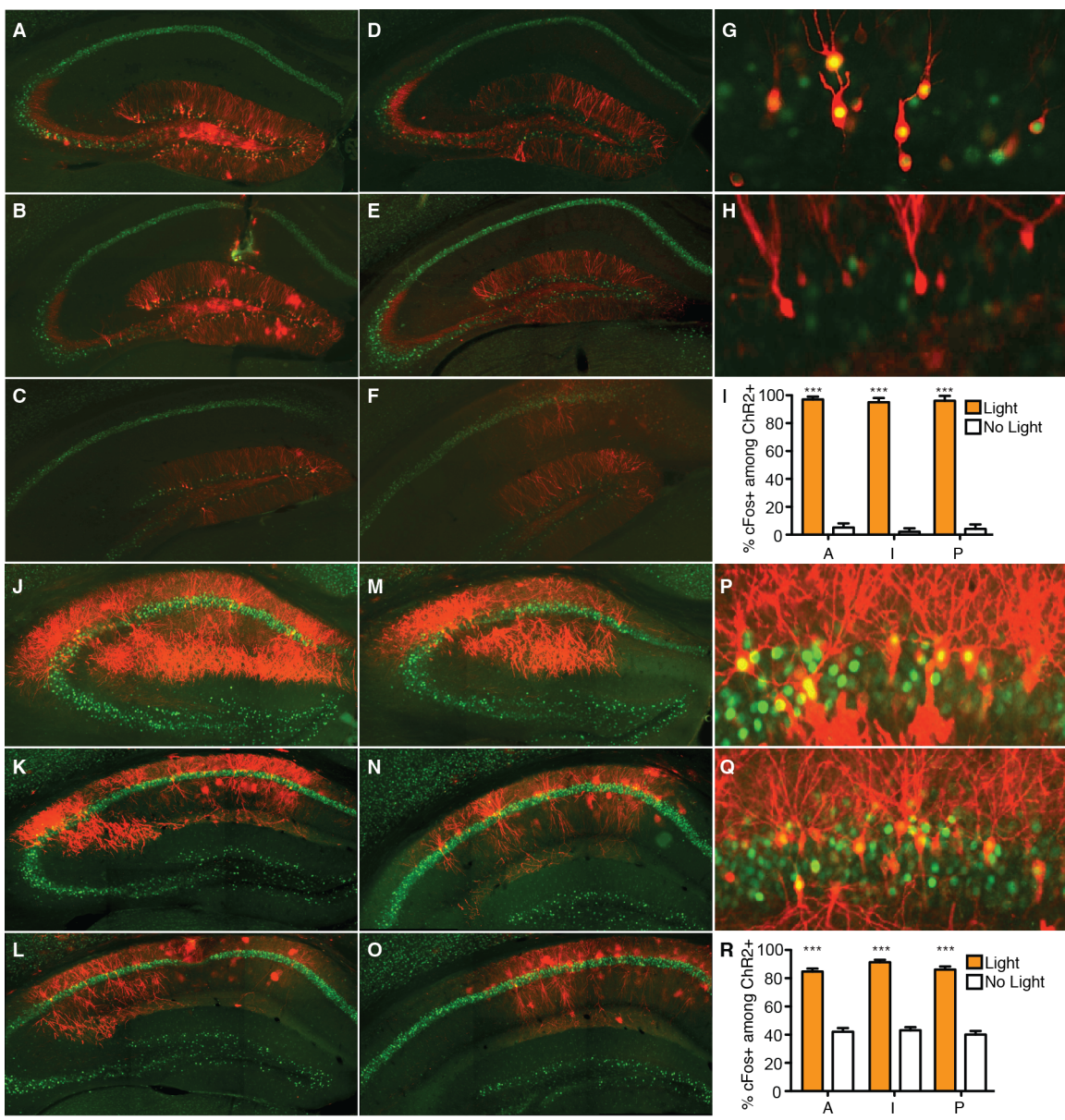


Fig. S1. Light stimulation induced cFos expression in ChR2+ cells throughout DG or CA1. (A–I) Animals expressing ChR2-mCherry (red) in the DG were treated with or without light stimulation and the expression of cFos (green) was examined. Representative anterior, intermediate, posterior, and higher magnification images of DG for the light stimulated group (A, B, C, and G) and no light group (D, E, F, and H) are shown. Quantification of cFos positive cells among ChR2 positive cells is shown in (I). A: anterior, I: intermediate, P: posterior. ($n = 3/\text{group}$; *** $P < 0.001$). (J–R) The same as A–I, except the ChR2-mCherry is expressed in CA1.

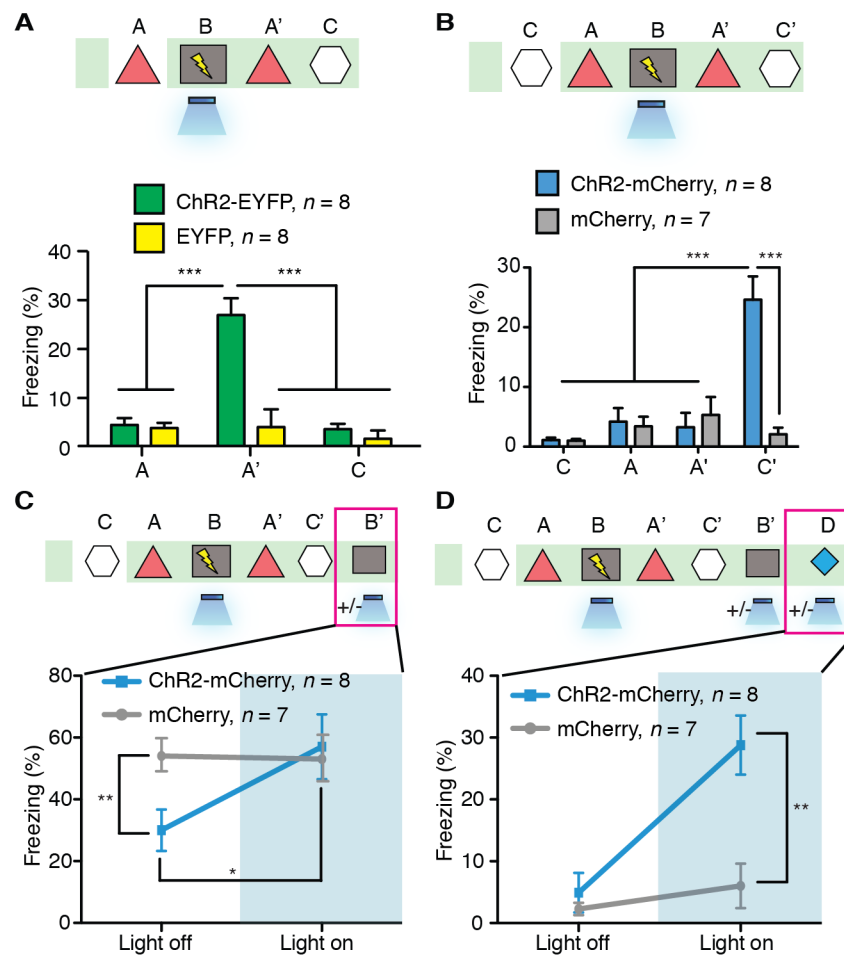


Fig. S2. Formation of false memory is reproducible under various conditions.

(A) Top: c-fos-tTA animals injected with AAV₉-TRE-ChR2-EYFP or AAV₉-TRE-EYFP in DG underwent training and testing shown. Bottom: animals' freezing levels in context A before fear conditioning and in context A and C after fear conditioning ($n = 8$ for each group; *** $P < 0.001$). (B) The c-fos-tTA animals injected with AAV₉-TRE-ChR2-mCherry or AAV₉-TRE-mCherry in DG that underwent the behavioral protocol shown above. The freezing levels for each session are shown ($n = 8$ for ChR2-mCherry group and $n = 7$ for mCherry group; *** $P < 0.001$). (C and D) The same animals from B were re-exposed to context B (C) and context D (D). The freezing levels were examined both in the absence and presence of light stimulation. (* $P < 0.05$; ** $P < 0.01$).

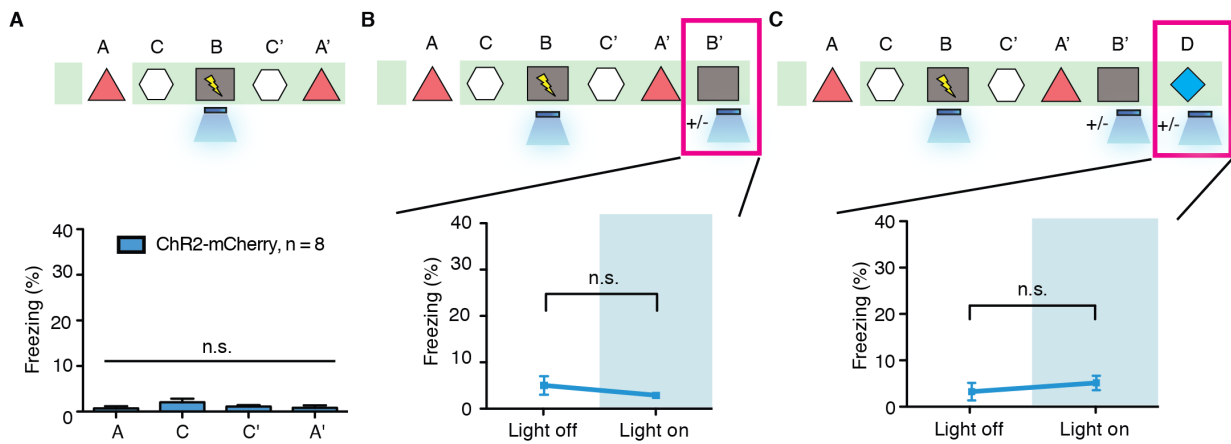


Fig. S3. Animals undergoing an immediate shock protocol with light stimulation do not form a false fear memory.

(A) The c-fos-tTA animals injected with AAV₉-TRE-ChR2-mCherry in the DG underwent the behavioral protocol shown above and their freezing levels for each session are shown below ($n = 8$ for ChR2-mCherry). (B and C) The same animals were re-exposed to context B and context D. Freezing levels were examined both in the absence and presence of light stimulation. (n.s.: not significant).

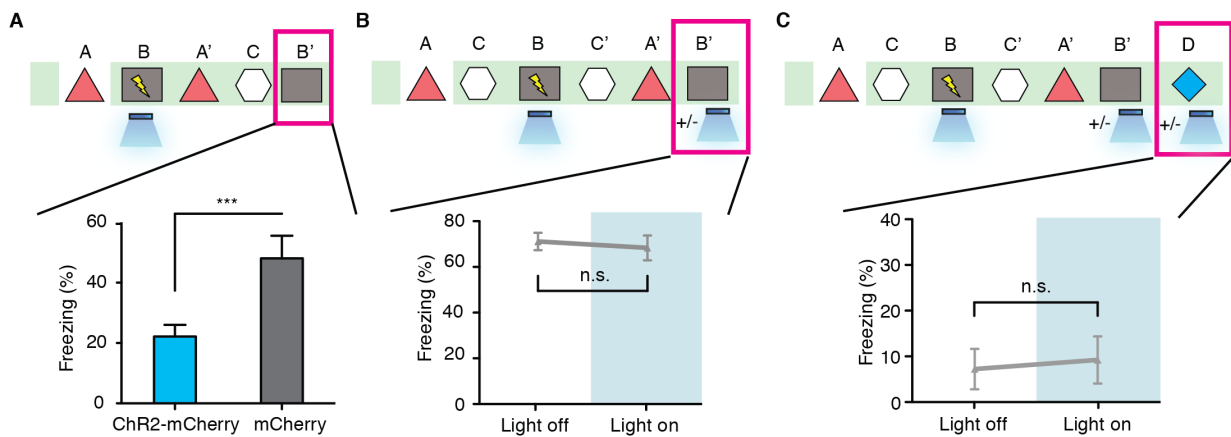


Fig. S4. False memory formation interfered with genuine memory recall.

(A) The c-fos-tTA animals injected with AAV₉-TRE-ChR2-mCherry or AAV₉-TRE-mCherry in DG that underwent the behavioral protocol shown above were re-exposed to context B and the freezing levels were measured. ($n = 8$ for ChR2-mCherry group and $n = 6$ for mCherry group; *** $P < 0.001$). (B and C) The c-fos-tTA animals injected with AAV₉-TRE-mCherry in DG that underwent the behavioral protocol shown above were re-exposed to context B (B) and context D (C). The freezing levels were examined both in the absence and presence of light stimulation. ($n = 6$; n.s.: not significant).

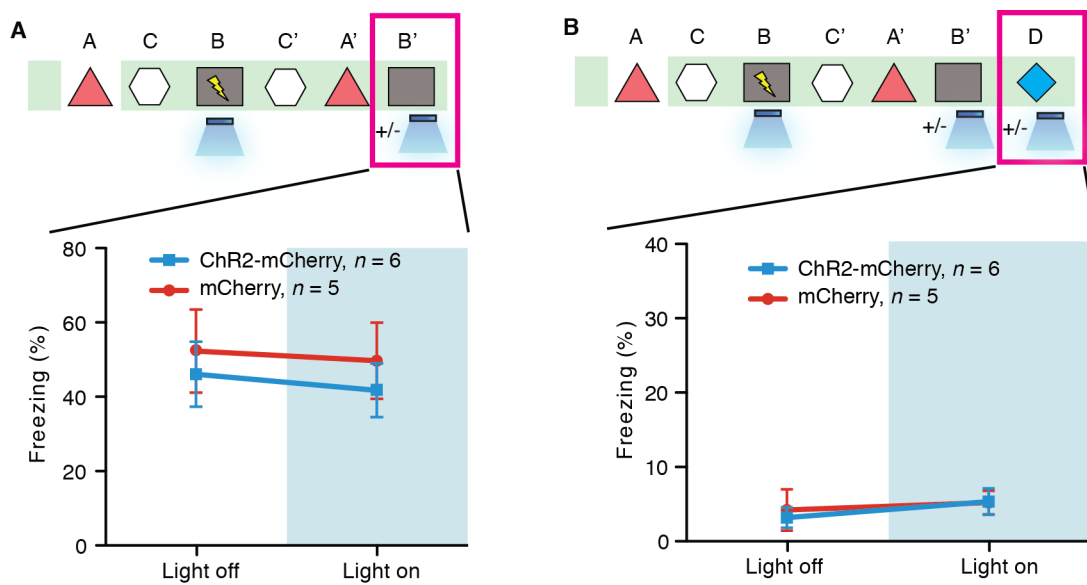


Fig. S5. Fear memory tests for CA1 animals in context B and context D.

The c-fos-tTA animals injected with AAV₉-TRE-ChR2-mCherry or AAV₉-TRE-mCherry in CA1 that underwent the behavioral protocol shown above were re-exposed to context B (**A**) and context D (**B**). The freezing levels were examined both in the absence and presence of light stimulation. ($n = 6$ for ChR2-mCherry group and $n = 5$ for mCherry group).

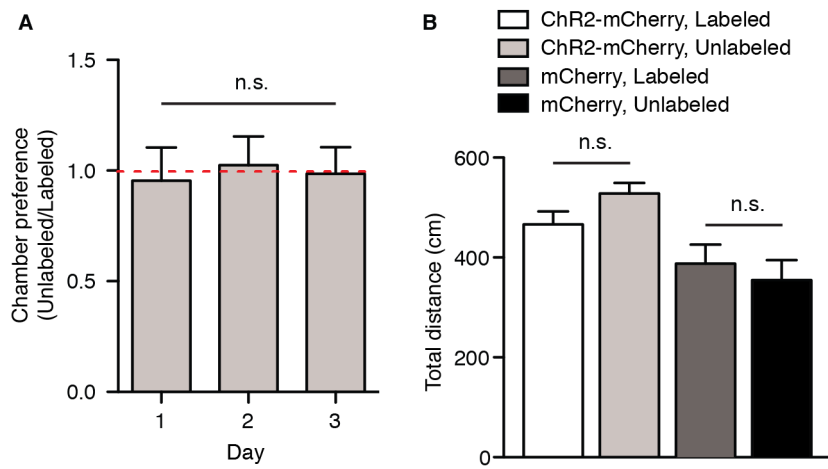


Fig. S6. Control data for the CPA experiments.

(A) A group of wild-type mice were exposed to the CPA apparatus and allowed to explore both chambers freely for 3 consecutive days. Their preferences for the chambers were measured as a ratio of time spent in each chamber during each day ($n = 6$). (B) The c-fos-tTA animals injected with either AAV₉-TRE-ChR2-mCherry or AAV₉-TRE-mCherry in DG were taken off Dox and exposed to one chamber (Labeled) of the CPA apparatus, then put back on Dox and exposed to the other chamber (Unlabeled) the next day. Total distances traveled for each exposure were shown for each chamber for both groups ($n = 8$ for each group).

References

- S1. L.G. Reijmers, B.L. Perkins, N. Matsuo, M. Mayford, *Science* **317**, 1230–1233 (2007).
- S2. X. Liu *et al.*, *Nature* **484**, 381–385 (2012).
- S3. G. Paxinos, K. Franklin, *The Mouse Brain in Stereotaxic Coordinates* (Academic Press, 2001).
- S4. C.A. Schneider, W.S. Rasband, K.W. Eliceiri, *Nat. Methods* **9**, 671–675 (2012).